Human Pathology (2019) **83**, 77–89

ELSEVIER

Human PATHOLOGY

www.elsevier.com/locate/humpath

Original contribution

Immunohistochemical characterization of cancer-associated fibroblasts at the primary sites and in the metastatic lymph nodes of human intrahepatic cholangiocarcinoma☆,☆☆

Rei Atono Itou MD[a], Naoki Uyama MD, PhD[a,*], Seiichi Hirota MD, PhD[b], Norifumi Kawada MD, PhD[c], Songtao Wu MD[a], Seikan Miyashita MD, PhD[a], Ikuo Nakamura MD, PhD[a], Kazuhiro Suzumura MD, PhD[a], Hideaki Sueoka MD, PhD[a], Tosihiro Okada MD, PhD[a], Etsuro Hatano MD, PhD[a], Hiroko Tsutsui MD, PhD[a], Jiro Fujimoto MD, PhD[a]

[a]*Department of Surgery, Hyogo College of Medicine, Hyogo 663-8501, Japan*
[b]*Department of Surgical Pathology, Hyogo College of Medicine, Hyogo 663-8501, Japan*
[c]*Department of Hepatology, Graduate School of Medicine, Osaka City University, Osaka 558-8585, Japan*

Received 1 May 2018; revised 14 August 2018; accepted 16 August 2018

Keywords:
Intrahepatic cholangiocarcinoma;
Cancer-associated fibroblasts;
Hepatic stellate cells;
Portal fibroblasts;
Bone marrow–derived fibrocytes

Summary Cancer-associated fibroblasts (CAFs) are an important constituent of the cancer stroma. In intrahepatic cholangiocarcinoma (ICC), the features of CAFs at the primary site and in the metastatic lymph nodes (Met-LNs) and their origin have been unclear. In the present study, we characterized CAFs at the primary site (n = 42) and in the Met-LNs (n = 10) of human ICC by immunohistochemistry using potential molecular markers of CAFs, portal fibroblasts (PFs), hepatic stellate cells (HSCs), and bone marrow–derived fibrocytes (BMDFs). At the primary site, the stroma was strongly positive for α-smooth muscle actin (α-SMA; marker for CAFs), platelet-derived growth factor receptor-β (PDGFR-β) (common marker for HSCs and PFs), fibulin-2, and thymus cell antigen-1 (Thy-1; PF marker), whereas immunoreactivity for fascin (HSC marker) was scarce. Most of the α-SMA–positive cells were found to express PDGFR-β, Thy-1, and fibulin-2 by double immunostaining. A small population of BMDF marker–positive (α-SMA$^+$ CD45$^+$CD34$^+$) cells was found by triple immunostaining. In the micro–Met-LNs, α-SMA–positive cells were absent in cancer aggregates of the LN sinus, whereas they were present in the invasion area of cancer cells from the LN sinus to the LN parenchyma. In the macro–Met-LNs, there were abundant α-SMA–positive cells that were also positive for PDGFR-β and Thy-1 but negative for fibulin-2 and fascin. Thus,

Abbreviations: ICC, intrahepatic cholangiocarcinoma; CAF, cancer-associated fibroblast; PF, portal fibroblast; HSC, hepatic stellate cell; BMDF, bone marrow–derived fibrocyte; LN, lymph node; α-SMA, α-smooth muscle actin; PDGFR, platelet-derived growth factor receptor; Thy-1, thymus cell antigen-1; PBS, phosphate-buffered saline.

☆ Competing interest: The authors declare that they have no conflict of interest.

☆☆ Funding/Support: This study was supported by JSPS Grant-in-Aid for Scientific Research (C) (KAKENHI 26462051) and Grant-in-Aid for Researchers, Hyogo College of Medicine, 2016.

* Corresponding author at: Department of Surgery, Hyogo College of Medicine, Mukogawacho 1-1, Nishinomiya, Hyogo 663-8501, Japan.
E-mail address: amanetask@gmail.com (N. Uyama).

https://doi.org/10.1016/j.humpath.2018.08.016

regarding the expression of molecular markers, CAFs at the primary site of ICC are similar to PFs and different from those of HSCs or CAFs in the Met-LNs. CAFs at the primary sites and in the Met-LN are thought to be derived from PFs/BMDFs and resident cells of LNs, respectively.

1. Introduction

ICC accounts for at least 10% of primary liver cancers, and its incidence has consistently increased over the last decade [1]. ICC is considered a malignant disease with a poor prognosis, and cases with LN metastasis have a particularly poor prognosis [2]. Histologically, ICC is similar to pancreatic ductal adenocarcinoma, being characterized by an abundant desmoplastic stroma consisting of immune cells, fibroblasts, blood vessels, and extracellular matrix materials, such as fibril-forming collagens [3-5].

Among the cellular components of the stroma, substantial attention has been paid to CAFs in recent years. In 1979, cells with morphologic and molecular properties of myofibroblasts were reported to be present in the stroma of solid tumors and were referred to as CAFs [6]. CAFs usually express α-SMA, which is widely used as a marker for myofibroblasts. In addition, they are reported to express fibroblast-activating protein, neuron glial antigen-2, vimentin, PDGFR-β, and prolyl-4-hydroxylase [7-10]. The presence of CAFs is thought to be related to the development of high-grade malignancies, metastasis, and a poor prognosis in breast cancer [11-13]. They were also reported to promote tumor growth, angiogenesis, and tumor invasion by the production of various cytokines and growth factors [7,8,11-13]. In ICC, it has been reported that the expression of α-SMA and PDGFR-β by CAFs is correlated with the prognosis and that CAFs regulate the ability of cancer cells to invade and metastasize by the production of hepatocyte growth factor, stromal cell–derived factor-1, and tenascin-C [4]. They are also reported to induce resistance of cancer cells to apoptosis by the production of periostin [4].

Generally, cellular sources of CAFs are thought to be resident cells, such as fibroblasts, pericytes, smooth muscle cells, and bone marrow–derived cells. In the liver, PFs, HSCs, and bone marrow–derived cells are cellular sources of myofibroblats [8,13,14]. PFs and activated HSCs express α-SMA and PDGFR-β commonly [15]. In contrast, Thy-1, fibulin-2, fascin, and cytoglobin have been reported as markers for distinguishing PFs from HSCs; Thy-1 and fibulin-2 are expressed by PFs [16], whereas fascin and cytoglobin are expressed by HSCs [17]. Isolated BMDFs express CD34 (the hematopoietic progenitor cell antigen marker), CD45 (the common leukocyte marker), collagen type I, and vimentin. When BMDFs differentiate into myofibroblast-type cells in damaged organs, the expression of α-SMA, fibronectin, and collagen type I is induced, whereas the expression of CD34 and CD45 is gradually reduced [18]. As for CAFs in human ICC, HSCs have been thought of as the dominant cellular source of CAFs [19,20], although detailed analyses are lacking.

Several reports have confirmed the presence of CAFs in metastatic LNs (Met-LNs) and their immunohistologic features in some cancers [21-25]. Yeung et al [26] showed the presence of α-SMA–immunoreactive fibroblasts in the stroma of Met-LNs of colorectal cancer. Matsuwaki et al [21] reported a similar expression of podoplanin in CAFs at the primary site and Met-LNs of lung cancer. The similar expression of RhoA, Rac1, α-SMA, and S100A4 in CAFs between primary sites and Met-LNs of breast cancer was also reported [23,24]. These reports suggested that a similar cancer microenvironment is maintained at metastatic sites. However, the presence and histologic features of CAFs in the Met-LNs of ICC have been unclear.

In the present study, we characterized CAFs at the primary sites of human ICC (ICC-CAFs) by immunohistochemistry with the molecular markers of PFs, HSCs, and BMDFs. In addition, we revealed the presence and the histologic features of CAFs in the Met-LNs (Met-LN-CAFs). Accordingly, we discussed possible cellular sources of ICC-CAFs and Met-LN-CAFs.

2. Materials and methods

2.1. Human liver tissues and Met-LNs

Specimens of ICC, noncancerous liver, and Met-LNs were collected during hepatectomies at the Hyogo College of Medicine (Nishinomiya, Hyogo, Japan). Hepatectomy was performed for 46 patients with ICC between January 2005 and December 2014. The tissues of 4 primary sites were inadequately preserved and could not be used for the present study. LN sampling was performed in 36 of 46 patients, and the Met-LNs of 10 patients were used for the present study.

All research protocols of this study were approved by the Ethics Committee of Hyogo College of Medicine (approval number 201707-017). All research projects were in compliance with the terms of the 1964 Declaration of Helsinki and its later amendments or comparable ethical standards. We obtained informed consent from human subjects.

2.2. Immunostaining of human liver tissues and LNs

Tissue specimens were fixed for 48 hours in 10% buffered formalin and embedded in paraffin wax before sectioning. Sections of 4-μm thickness for each specimen were prepared

on silanized slides (Agilent Technologies, Tokyo, Japan). For immunohistochemistry, the paraffin sections were dewaxed in xylene and rehydrated in decreasing concentrations of ethanol (xylene, 3 × 5 minutes; 99% ethanol, 2 × 3 minutes; 95% ethanol, 3 minutes; 70% ethanol, 3 minutes). The sections were treated with 0.3% H_2O_2 in 100% methanol for 30 minutes at room temperature to block endogenous peroxidase activity. Antigen retrieval was performed by exposing slides to microwave heating for 40 minutes at 95°C in 0.01 M citrate buffer (pH 6.0).

The sections were then preincubated with serum-free protein block (Agilent Technologies) for 30 minutes at room temperature. Primary antibodies (Supplementary Table S1) were diluted in PBS and then added to each slide overnight at 4°C. The slides were washed 3 times in PBS for 5 minutes. Secondary antibody staining was performed using the Dako EnVision+ kit (Agilent Technologies) according to the manufacturer's instructions. The slides were then washed 3 times with PBS for 5 minutes, incubated with 3, 3′-diaminobenzidine–H_2O_2 mixture for another 20 minutes, rinsed with distilled water, and counterstained with hematoxylin. The sections were dehydrated with an ethanol series followed by xylene and mounted using Malinol (Muto Pure Chemicals, Tokyo, Japan). The staining was visualized under a Nikon Eclipse TS-100 microscope (Nikon, Tokyo, Japan). Immunoreactivity for PF markers and an HSC marker at the primary sites and the Met-LN of ICC was scored as follows: negative (−), when positive cells were 0% of the stroma cells; very weakly positive (±), when positive cells were less than 10% of the stroma cells; weakly positive (+), when positive cells were 10% to 50% of the stroma cells; strongly positive (++), when positive cells were 50% to 80% of the stroma cells; and very strongly positive (+++), when positive cells were greater than 80% of the stroma cells.

2.3. Immunofluorescent staining with confocal microscopy

To characterize α-SMA–immunoreactive cells or fascin-immunoreactive cells, double fluorescent immunostaining for α-SMA or fascin with other markers was performed. In addition, to investigate the presence of BMDFs in the stroma at the primary site, triple fluorescent immunostaining of α-SMA, CD34, and CD45 was performed. Fluorochrome labeling was viewed under a Zeiss Axiovert LSM510 confocal microscope and documented using the LSM510 software program (Carl Zeiss, Tokyo, Japan).

3. Results

3.1. Expression of molecular markers of PFs and HSCs in noncancerous liver tissues

First, the expression of α-SMA, PDGFR-β, Thy-1, fibulin-2, and fascin was investigated in normal human liver tissues (Supplementary Fig. S1). Immunoreactivity for α-SMA and PDGFR-β was found in the periportal area and along the hepatic sinusoids (Supplementary Fig. S1A-C and D-F). Immunoreactivity for Thy-1 and fibulin-2 was present only at the periportal area and not in the sinusoidal area (Supplementary Fig. S1G-I and J-L), whereas fascin immunoreactivity was found exclusively along the sinusoid and not in the periportal area (Supplementary Fig. S1M-O). Based on these observations, in addition to those in previous reports [15-17,27], we defined α-SMA and PDGFR-β as common markers of PFs and activated HSCs, Thy-1 and fibulin-2 as PF markers, and fascin as an HSC marker in this study.

Next, we also performed immunohistochemistry for α-SMA, Thy-1, fibulin-2, and fascin in human cirrhotic liver (Supplementary Fig. S2). Immunoreactivity for α-SMA (Supplementary Fig. S2A-C) was found in the fibrotic septa (Supplementary Fig. S2B) and along the hepatic sinusoids (Supplementary Fig. S2C). As for Thy-1 (Supplementary Fig. S2D-F) and fibulin-2 (Supplementary Fig. S2G-I), immunoreactivity was found in the fibrotic septa (Supplementary Fig. S2E and H) but not in the sinusoidal area (Supplementary Fig. S2F and I). On the other hand, fascin immunoreactivity was found in the sinusoidal area (Supplementary Fig. S2L) but not in the fibrotic septa (Supplementary Fig. S2K). From these data, in human cirrhotic liver, PFs may contribute to the production of fibrotic septa, whereas HSCs may contribute to the production of pericellular fibrosis.

3.2. Expression of molecular markers of PFs, HSCs, and BMDFs in CAFs at the primary sites of ICC

Next, the expression of the above-mentioned molecular markers was investigated in the stroma of ICC by immunohistochemistry. Immunohistochemistry for α-SMA was first performed because α-SMA is thought to be a marker of CAFs in addition to PFs and HSCs. Immunoreactivity for α-SMA (Fig. 1A and B) was found in the stroma of all specimens, and its strong immunoreactivity (++ or +++) was found in 40 (95.2%) specimens of 42 ICC cases (Table 1). These data suggest that CAFs may be present in the stroma of ICC and that α-SMA is a useful marker of ICC-CAFs. Reactivity of PDGFR-β, a common marker of PFs and HSCs, was found in all specimens (Fig. 1C and D), and its strong immunoreactivity (++ or +++) was found in 14 (33.3%) specimens (Table 1). To confirm the expression of PDGFR-β by ICC-CAFs, double immunostaining of PDGFR-β and α-SMA was performed. The immunoreactivity for PDGFR-β clearly overlapped with that for α-SMA (Fig. 2A-C), indicating that PDGFR-β is expressed by ICC-CAFs.

In addition, we investigated the expression of individual PF markers and an HSC marker in the ICC stroma by immunohistochemistry. In the stroma at primary sites, immunoreactivity for Thy-1 (Fig. 1E and F) and fibulin-2 (Fig. 1G and H) was found in all specimens and 29 (69.0%) specimens, respectively. Strong immunoreactivity (++ or +++) for Thy-1 and fibulin-2 was found in 39 (92.9%) and 11 (26.2%) specimens,

respectively (Table 1). To confirm these markers' expression by CAFs, double immunofluorescent staining was performed. Immunoreactivity for α-SMA overlapped with that of Thy-1 (Fig. 2D-F) or fibulin-2 (Fig. 2G-I), indicating that ICC-CAFs are positive for Thy-1 and fibulin-2.

In most specimens, immunoreactivity for fascin was found in cancer cells but not in most stromal cells (Fig. 1I and J). In 26 (61.9%) specimens, scarce immunoreactivity for fascin was found in a limited area of the stroma. To characterize fascin-positive cells in the ICC stroma, double immunofluorescent

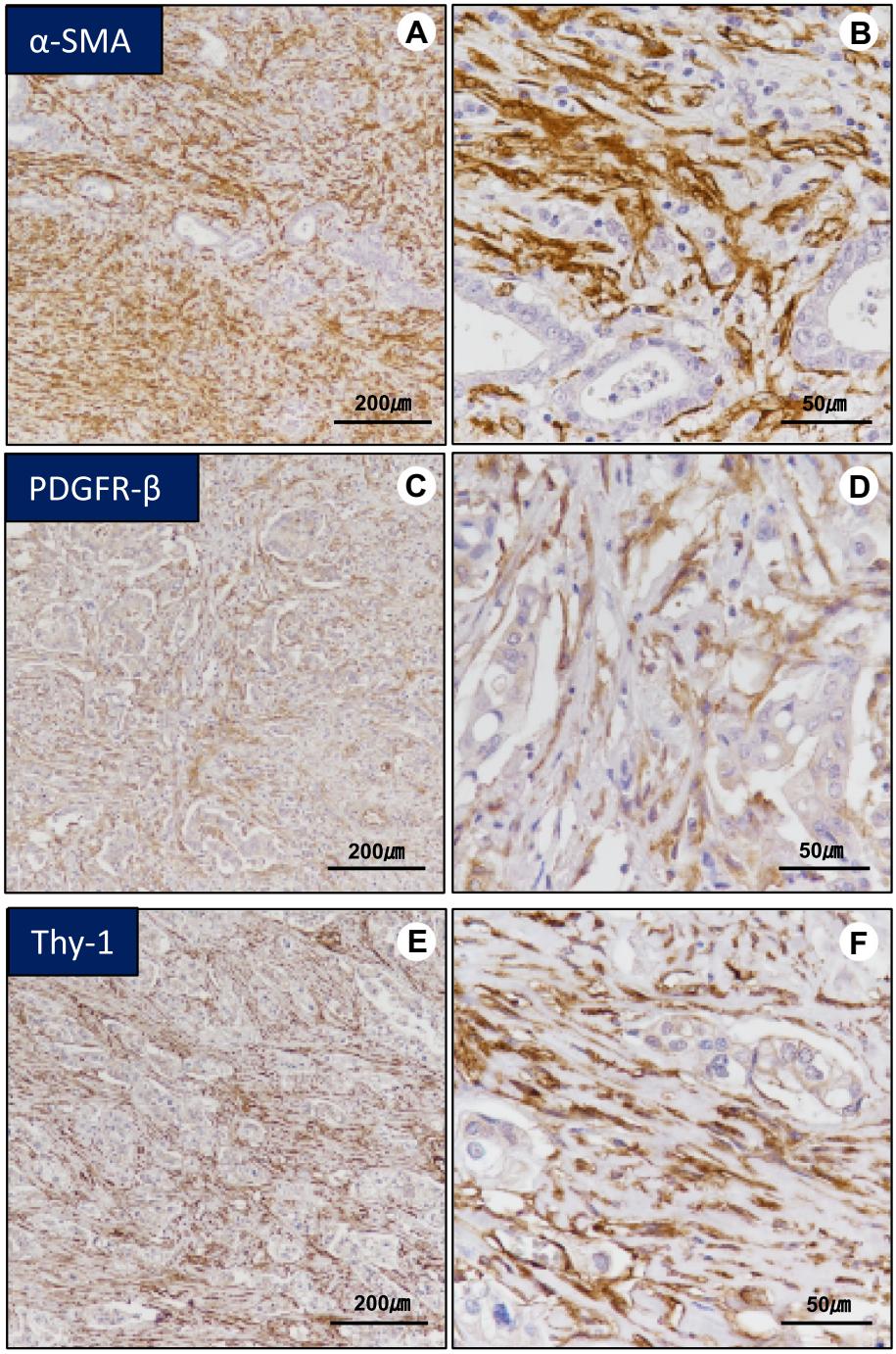

Fig. 1 Immunostaining for α-SMA (A and B), PDGFR-β (C and D), Thy-1 (E and F), fibulin-2 (G and H), and fascin (I and J) in the stroma of ICC tissues. α-SMA is a CAF marker as well as a common marker of PFs and HSCs. PDGFR-β is a common marker of PFs and HSCs, Thy-1 and fibulin-2 are PF markers, and fascin is an HSC marker. Immunoreactivity for α-SMA, PDGFR-β, Thy-1, and fibulin-2 was found in the stroma. Immunoreactivity for fascin was found in cancer cells (arrows), whereas it was scarce in the stroma of primary sites. Original magnifications ×100 (A, C, E, G, and I) and ×400 (B, D, F, H, and J).

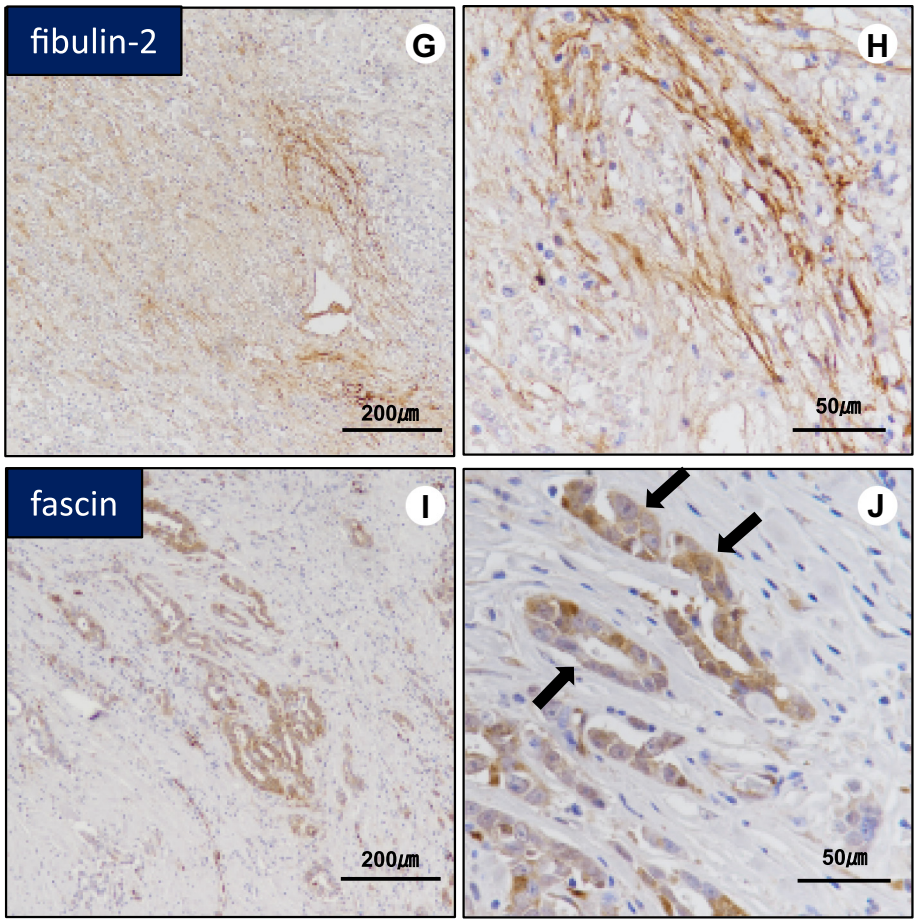

Fig. 1. (*continued*).

staining for fascin with α-SMA (Fig. 3A-C), Thy-1 (Fig. 3D-F), or fibulin-2 (Fig. 3G-I) was performed. Fascin immunoreactivity clearly overlapped with that of α-SMA, Thy-1, and fibulin-2, suggesting that small populations of ICC-CAFs may be derived from cells with characteristics of PFs and HSCs.

To investigate the presence of BMDFs in noncancerous liver and ICC, triple immunostaining of α-SMA, CD34, and CD45 was performed. At the periportal area (Supplementary Fig. S3A-D) of normal human liver, immunoreactivity for α-SMA (Supplementary Fig. S3 A) did not overlap with that of CD34 (Supplementary Fig. S3B) or CD45 (Supplementary Fig. S3C), except for vessels such as hepatic artery and portal vein (Supplementary Fig. S3D). Immunoreactivity of α-SMA and CD34 was very close at the hepatic artery and portal vein of the periportal area. In the sinusoidal area (Supplementary Fig. S3E-H), immunoreactivity for CD34 was very weak and immunoreactivity for α-SMA (Supplementary Fig. S3E) did not overlap with that of CD34 (Supplementary Fig. S3F) or CD45 (Supplementary Fig. S3G). Also in cirrhotic liver (Supplementary Fig. S3I-L), immunoreactivity for α-SMA (Supplementary Fig. S3I) was not overlapping with that of D34 (Supplementary Fig. S3J) or CD45 (Supplementary Fig. S3K) at the fibrotic septa (Supplementary Fig. S3L). Collectively, BMDFs may not contribute to fibroblastic cell population in normal and cirrhotic liver. On the other hand, in the stroma at primary sites of ICC, triple immunostaining of α-SMA (Fig. 4A, E, and I), CD34 (Fig. 4B, F, and J), and CD45 (Fig. 4C, G, and K) showed the presence of a small number of $CD34^{+}CD45^{+}\alpha\text{-}SMA^{+}$ cells (<1%; Fig. 4D, H, and L), suggesting that BMDFs may differentiate into myofibroblasts and contribute to some populations of ICC-CAFs.

Table 1 Expression of PFs and HSCs markers by CAFs in ICC

	PFs	HSCs	CAFs at the primary site	CAFs in the Met-LN
α-SMA	+++	+++	+++	++
PDGFR-β	++	++	++	+
Thy-1	++	−	+++	+
Fibulin-2	+	−	+	−
Fascin	−	+	±	−

NOTE. −, no positivity of CAFs in the stroma; ±, positivity of less than 10% cells of CAFs in the stroma; +, positivity of 10% to 50% of CAFs in the stroma; ++, positivity of 50% to 80% of CAFs in the stroma; +++, positivity of greater than 80% of CAFs in the stroma.

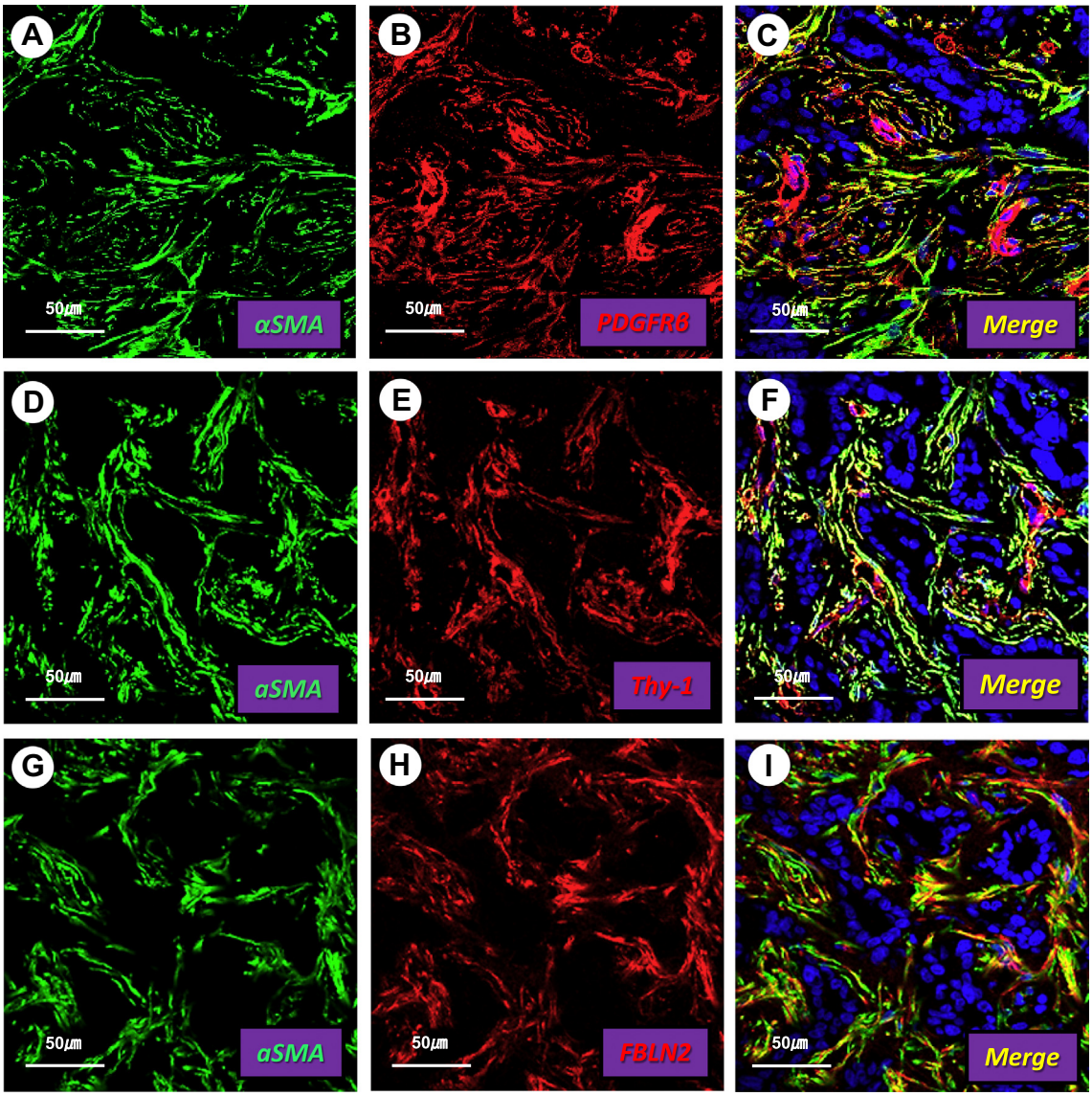

Fig. 2 Double immunofluorescent staining for α-SMA plus PDGFR-β (A-C), Thy-1 (D-F), or fibulin-2 (G-I) with confocal microscopy. α-SMA was labeled with Alexa 488 (green), whereas PDGFR-β, Thy-1, and fibulin-2 were labeled with Alexa 555 (red). Immunoreactivity for α-SMA clearly overlapped with that of PDGFR-β (C), Thy-1 (F), or fibulin-2 (I) (yellow), indicating that CAFs at the primary sites of ICC express PF markers, such as Thy-1 and fibulin-2, in addition to PDGFR-β. Original magnification is ×400.

3.3. Presence of CAFs in Met-LNs of ICC

To investigate the presence of Met-LN-CAFs, immunostaining for α-SMA was performed. In micro–Met-LNs, the aggregation of cancer cells in the LN sinus (Fig. 5A and B①) and microinvasion of cancer cells to the LN parenchyma were observed (Fig. 5A and C). α-SMA–positive cells were found around the LN sinus (Fig. 5B②) and in the parenchyma of LNs (Fig. 5C③); these cells might have been smooth muscle cells or pericytes of the LN sinus and fibroblastic reticular cells, respectively. In the aggregates of cancer cells of the LN sinus (Fig. 5B①), α-SMA–positive cells were absent, whereas some α-SMA–positive cells were found around cancer cells in the microinvasion area of the LN parenchyma (Fig. 5C④). These data suggest that Met-LN-CAFs in the microinvasion area may be derived from α-SMA–positive cells around the LN sinus and/or in the parenchyma.

In macro–Met-LNs, a large number of α-SMA–positive Met-LN-CAFs were present around cancer cells. There were 3 morphologic types of Met-LN-CAFs in aggregates. In one type, the Met-LN-CAFs encircled aggregated cancer cells (Fig. 5D and E), whereas in another type, they were disorderly present in the stroma, whose morphology was similar to that of the ICC-CAFs (Fig. 5F and G). We defined the former type as the encompassing type and the latter as the diffuse type. In the third type, both of the CAF morphologies mentioned above were found in the stroma, and we defined this as the mixed type. Among Met-LNs, we found encompassing type, diffuse type, and mixed type in 3, 3, and 4 specimens, respectively. In 6 of these 10 Met-LN specimens, tissues of primary sites were

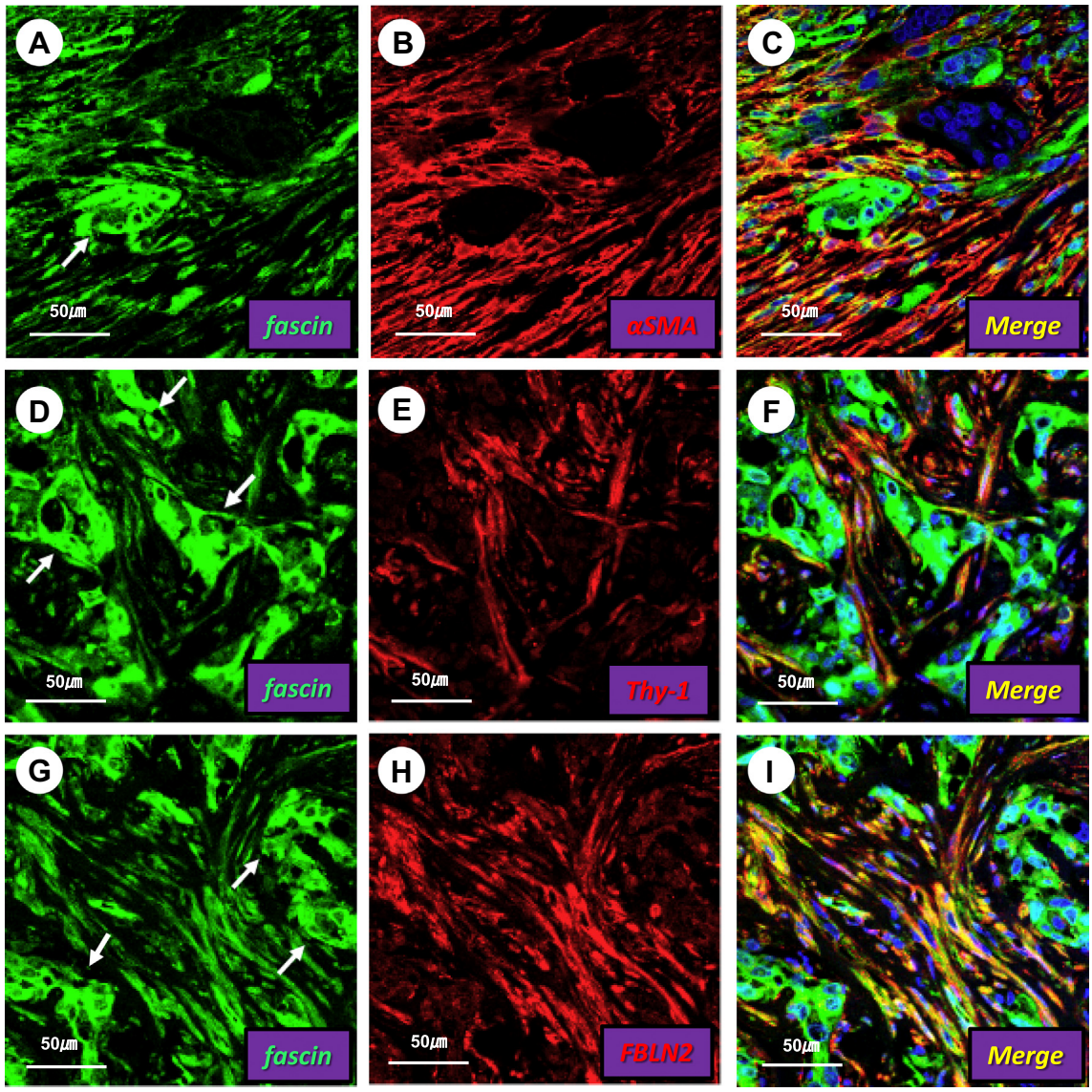

Fig. 3 Double immunofluorescent staining for fascin plus α-SMA (A-C), Thy-1 (D-F) or fibulin-2 (G-I) with confocal microscopy. Fascin was labeled with Alexa 488 (green), whereas α-SMA, Thy-1, and fibulin-2 were labeled with Alexa 555 (red). Immunoreactivity for fascin overlapped with that of α-SMA (C), Thy-1 (F), or fibulin-2 (I) (yellow). Fascin immunoreactivity was also found in cancer cells (arrows). These data indicate that fascin-positive cells in the stroma of primary site are CAFs and that they also express PF markers such as Thy-1 and fibulin-2. Original magnification ×400.

also preserved (encompassing type/diffuse type/mixed type, 1:2:3), and the morphologic types of CAFs at primary sites were all diffuse type.

3.4. Characterization of CAFs in Met-LNs with immunohistochemistry

Finally, we investigated the expression of molecular markers of PFs and HSCs in Met-LNs of ICC. Among the molecular markers of PFs and HSCs, immunoreactivity for α-SMA, PDGFR-β, and Thy-1 was found in all specimens (Fig. 6A-F). Immunoreactivity for fibulin-2 in the stroma of Met-LNs was not found in any specimens (Fig. 6G and H). In 6 cases whose primary sites and Met-LNs were preserved, the fibulin-2 expression in both areas was compared. In all specimens, the fibulin-2 expression was found in the stoma at the primary sites but not in that in the Met-LNs (Fig. 7A-D). Immunoreactivity for fascin was found in cancer cells but not in the cancer stroma of the Met-LNs of any specimens (Fig. 6I and J). These data indicate that the molecular expression pattern of Met-LN-CAFs differs from that of ICC-CAFs.

4. Discussion

In the present study, we first characterized ICC-CAFs by immunohistochemistry with molecular markers of CAFs, PFs, HSCs, and BMDFs. Our findings suggested that ICC-

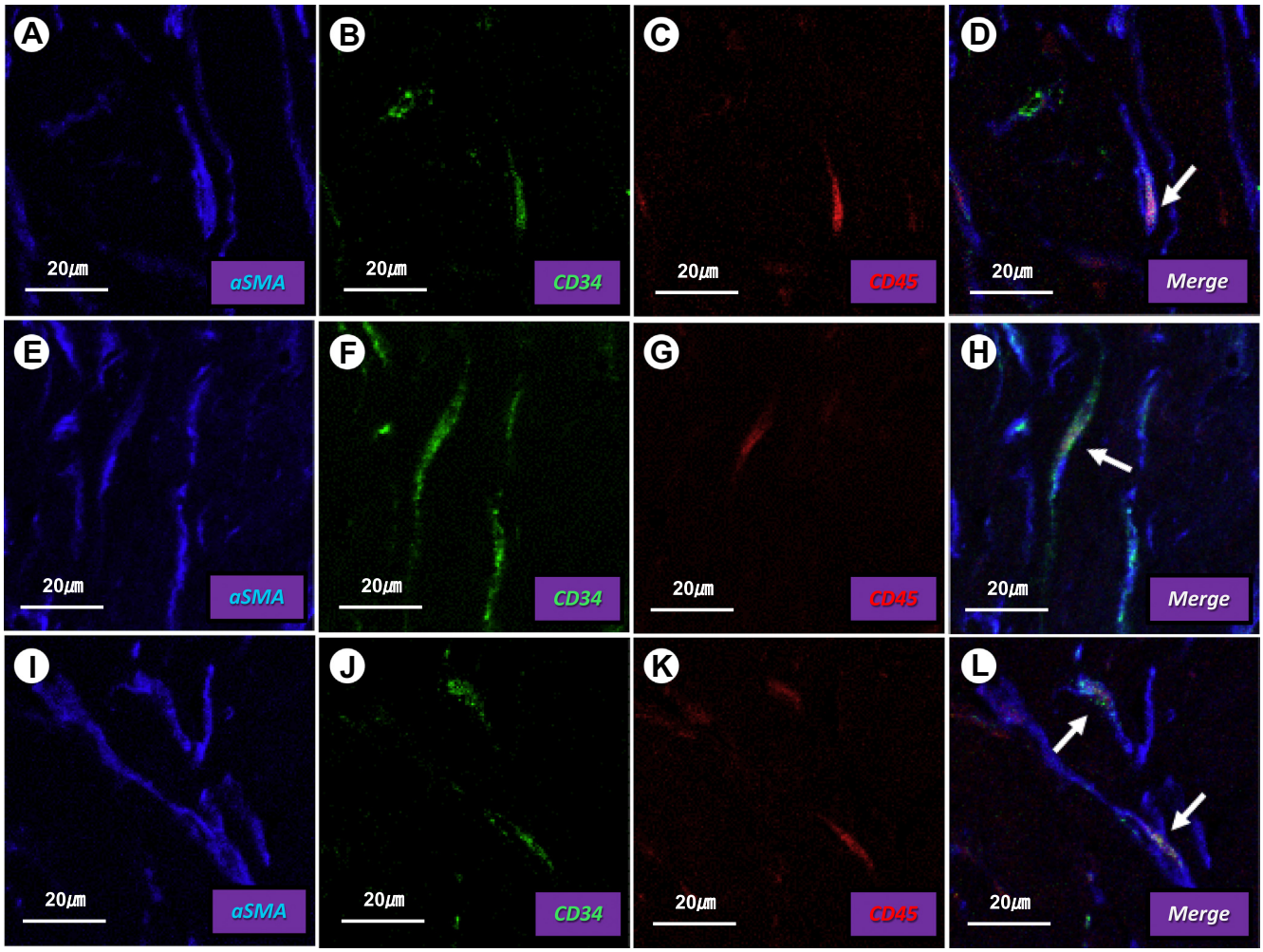

Fig. 4 Triple immunofluorescent staining for α-SMA (A, E, and I), CD34 (B, F, and J), and CD45 (C, G, and K) was performed and analyzed with confocal microscopy. α-SMA was labeled with Alexa 635 (blue), CD34 was labeled with Alexa 488 (green), and CD45 was labeled with Alexa 555 (red). Some α-SMA$^+$CD35$^+$CD45$^+$ cells (arrows) were found (D, H, and L) and were thought to be BMDFs. Original magnification ×1200.

CAFs might be derived from PFs and BMDFs because they predominantly expressed PF markers and a small number expressed BMDF markers. We then investigated the presence of CAFs and their morphology in the Met-LNs of ICC by immunostaining for α-SMA. At the microinvasion area of cancer cells in the micro–Met-LNs, there were only a few α-SMA–positive cells, whereas a lot of α-SMA–positive cells were present in the macro–Met-LNs. In addition, we showed 3 morphology types of Met-LN-CAFs in the macro–Met-LNs: the encompassing type, the diffuse type, and the mixed type. Finally, similar to the primary site, we characterized Met-LN-CAFs by immunohistochemistry. We found that the molecular expression pattern of Met-LN-CAFs was different from that of ICC-CAFs, suggesting that the cellular source of LN-CAFs may be from LN-resident fibroblastic cells and not from ICC-CAFs. This is the first report to characterize ICC-CAFs and Met-LN-CAFs with molecular markers of PFs and HSCs and to show the morphology of Met-LN-CAFs.

The cellular source of ICC-CAFs has been thought to be HSCs [19,20], although detailed analyses have not been performed. As mentioned in the Introduction section of this article, HSCs, PFs, and BMDFs have potential to contribute to the CAF population in ICC, as they can differentiate into resident myofibroblasts [8,10]. Therefore, immunohistochemistry with molecular markers of CAFs, PFs, HSCs, and BMDFs was performed. The immunostaining experiment showed that most ICC-CAFs expressed PF markers, such as Thy-1 (100%) and fibulin-2 (69.0%), whereas cells immunoreactive for fascin, an HSC marker, were scarce. These data indicate that most ICC-CAFs more closely resemble PFs than HSCs. In addition, interestingly, a small population of α-SMA$^+$CD34$^+$CD45$^+$ cells (<1%) was found in the stroma by confocal microscopy with triple immunostaining, suggesting that BMDFs may be another cellular source of ICC-CAFs. The origin of fascin-immunoreactive CAFs is unknown. We speculate that mesenchymal precursor cells, such as BMDFs, are their origin, as they also express PF markers such as Thy-1 and fibulin-2, although a detailed analysis was not performed. Further investigation will be necessary to clarify this issue.

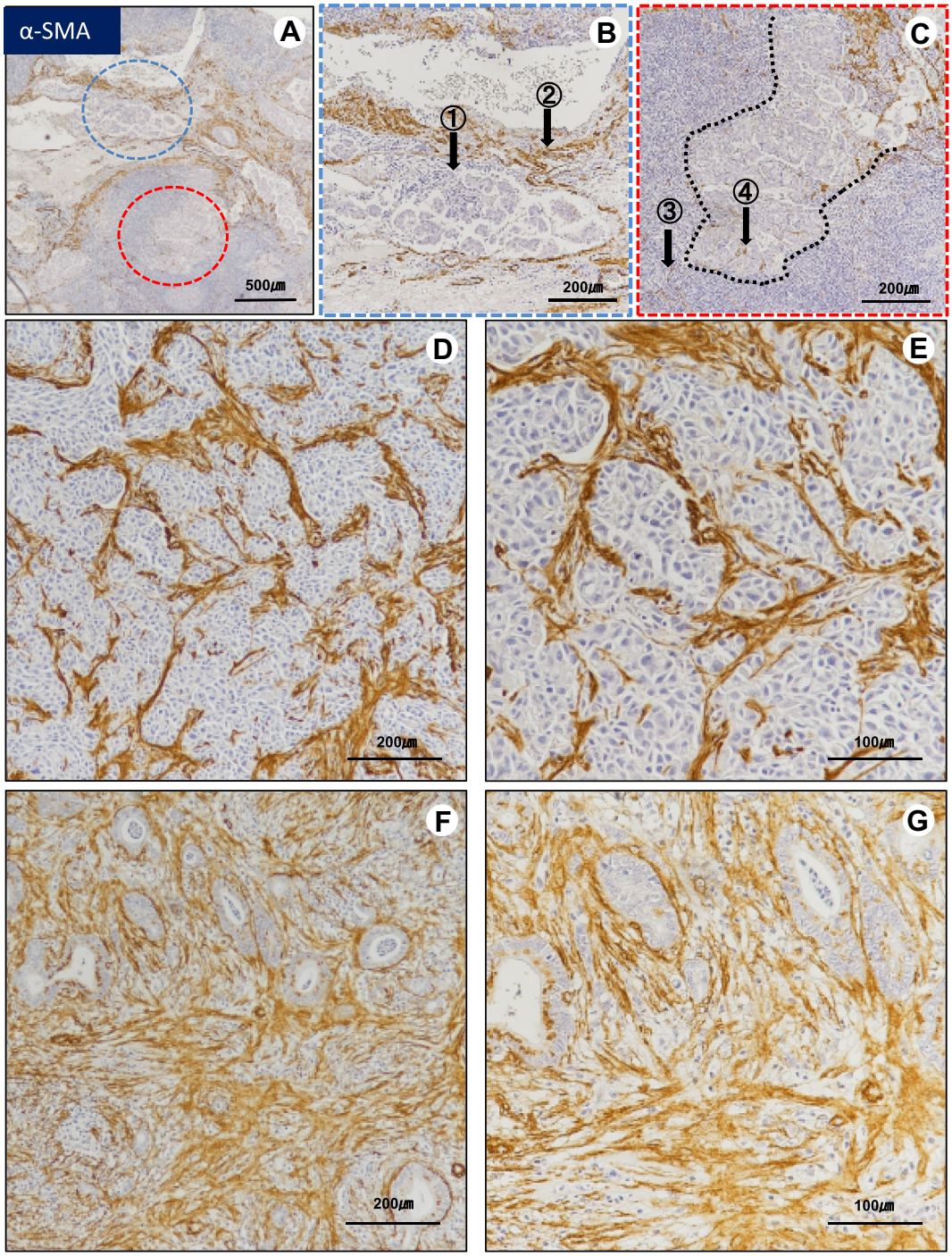

Fig. 5 Immunostaining for α-SMA in micro–Met-LNs (A-C) and macro–Met-LNs (D-G). A, In the micrometastatic area of LNs, the aggregation of cancer cells in the LN sinus (blue line circle) and the invasion of cancer cells into the parenchyma of the LNs (red line circle) were found. B, In the aggregate of cancer cells in the LN sinus, α-SMA–positive cells were not present (①). In the LNs, α-SMA–positive cells were present around the LN sinus (B②) and in the parenchyma (C③). C, In the microinvasion area, a small number of α-SMA–positive cells were found among the cancer cells (④). α-SMA–positive cells around the LN sinus and in the LN parenchyma were suspected to be smooth muscle cells or pericytes and fibroblastic reticular cells, respectively. D and F, In the macrometastatic area, there were 2 morphologic types of CAFs in aggregates. CAFs were present around the aggregates of cancer cells (the encompassing type: D and E) or diffusely present among cancer cells (the diffuse type: F and G). Original magnifications ×40 (A), ×100 (B, C, D, and F), and ×200 (E and G).

We next investigated the presence of Met-LN-CAFs of ICC. Regarding the metastatic process of cancer cells in LNs, they are thought to enter from imported lymph vessels to the peripheral LN sinuses, at which point they proliferate and invade the medullary space. The LN parenchyma is then gradually replaced with tumor cells [28]. A detailed analysis

of the presence of Met-LN-CAFs in ICC has not been reported. In the present study, we showed that α-SMA–immunoreactive cells were not found in an aggregate of cancer cells of the LN sinus. In addition, only a small number of α-SMA–immunoreactive cells were found in the area of micro-invasion to the LN parenchyma, whereas a lot of α-SMA–immunoreactive cells were found in macro–Met-LNs. These data suggest that Met-LN-CAFs of ICC may be derived from LN-resident cells rather than from primary sites. In the noncancerous area of LNs, α-SMA immunoreactivity was found around the LN sinus and in the LN parenchyma. The α-SMA immunoreactivity around the LN sinus is suspected

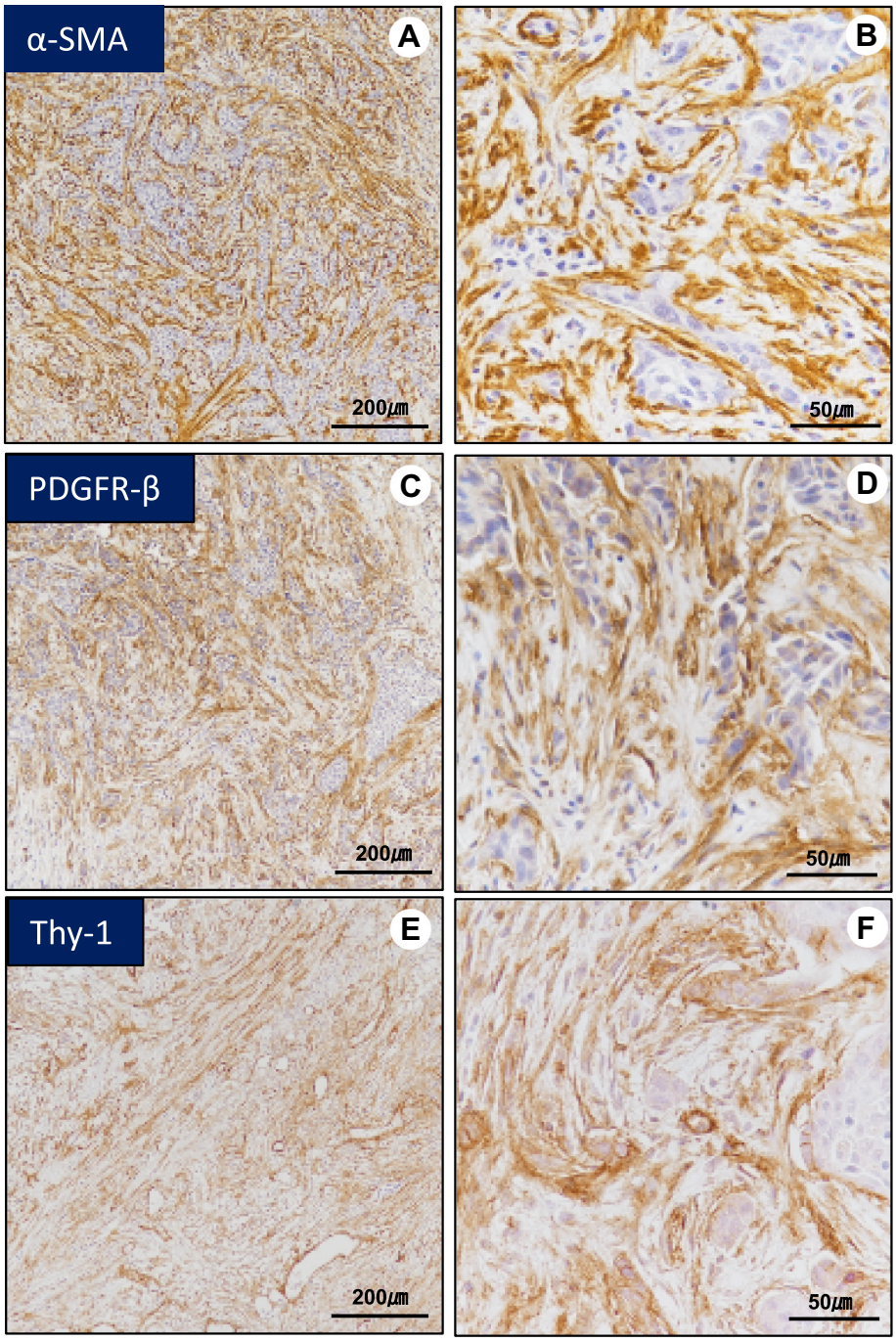

Fig. 6 Immunostaining for α-SMA (A and B), PDGFR-β (C and D), Thy-1 (E and F), fibulin-2 (G and H), and fascin (I and J) in the cancer stroma of Met-LNs. Immunoreactivity for α-SMA (A and B), PDGFR-β (C and D), and Thy-1 (E and F) but not for fibulin-2 (G and H) or fascin (I and J) was found in the cancer stroma of Met-LNs. Fascin immunoreactivity was found in cancer cells of Met-LNs (I and J). Original magnifications ×100 (A, C, E, G, and I) and ×400 (B, D, F, H, and J).

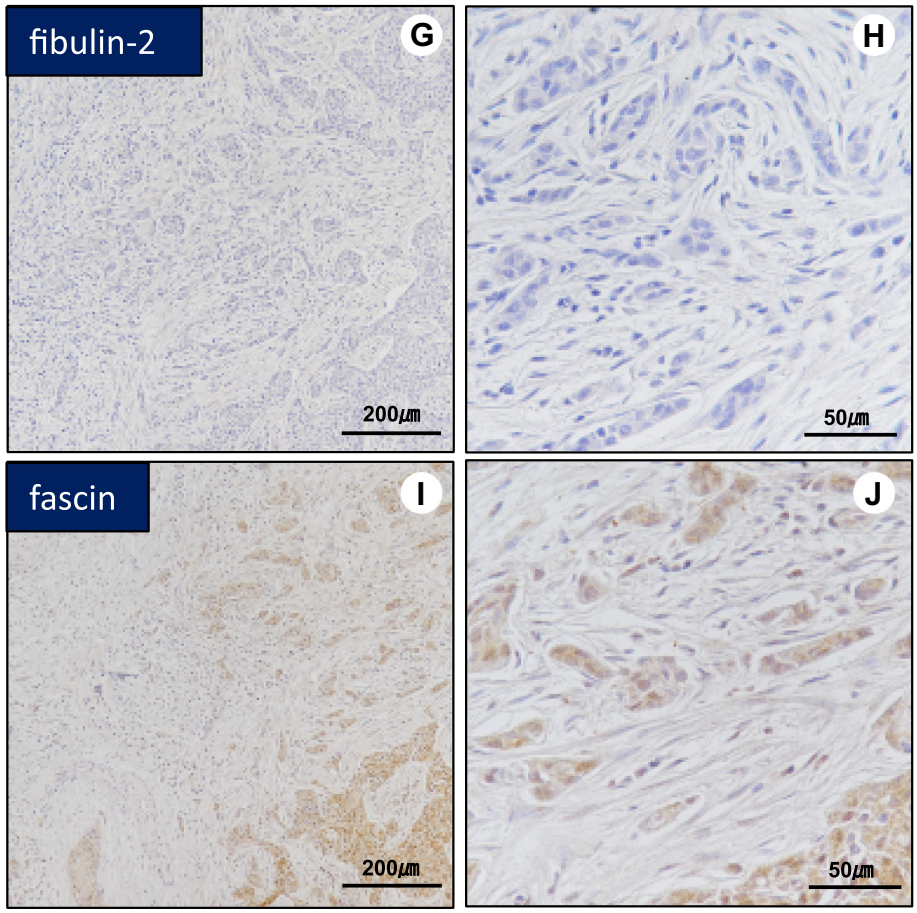

Fig. 6. (*continued*).

to be smooth muscle cells or pericytes, whereas that in the LN parenchyma is thought to be fibroblastic reticular cells; Met-LN-CAFs are speculated to be derived from these α-SMA–immunoreactive cells in LNs. However, a detailed analysis of fibroblastic cells in the LNs has not been performed, and the cellular source of Met-LN-CAFs remains obscure. Further investigations on cells with the potential to differentiate into CAFs in LNs are needed.

Regarding macro–Met-LNs, very interestingly, 3 morphologic types of CAFs in aggregates were found: the encompassing type, the diffuse type, and the mixed type. These findings raise 2 questions. The first question is, "Is the morphologic type of Met-LN-CAFs related to their malignant potential?" No study has yet addressed this question. In our cases, no significant difference in the patient survival was found among these types using the Kruskal-Wallis test ($P = .538$). However, we speculate that CAFs of the diffuse and mixed types may have more malignant potential than those of the encompassing type because the stroma of both the diffuse and mixed types was accompanied by desmoplastic reactions, although we have no evidence to support this idea. In addition, there was a disadvantage in this analysis in that the number of each group was small. Further investigation is thought to be necessary to answer this question. The second question is, "What causes these differences in morphologic type?" We did not precisely investigate this issue in the present study. To our knowledge, there is only one published article on growth factors related to desmoplastic stroma. In xenograft mouse models, a transforming growth factor β–transfected human pancreatic cancer cell line induced desmoplastic changes with increased matrix proteins [29]. Therefore, we speculate that growth factors and/or cytokines produced by cancer cells may affect the phenotype of CAFs. In the future, we will investigate the growth factors and/or cytokines involved in the desmoplastic reaction in the stroma of Met-LNs of ICC.

Several articles have described the characteristic features of Met-LN-CAFs, citing similar expression patterns between the primary sites and Met-LNs for molecular markers, such as CD31, podoplanin, α-SMA, and desmin in colorectal cancer [21]; RhoA, Rac1, α-SMA, and S100A4 in breast cancer [22,23]; and podoplanin in lung cancer [20]. In addition, Duda et al [25] reported that CAFs at the metastatic site may be derived from the stroma of the primary site based on their findings in a mouse GFP-positive skin graft model. Given these previous findings, we characterized Met-LN-CAFs by immunostaining with molecular markers of PFs and HSCs.

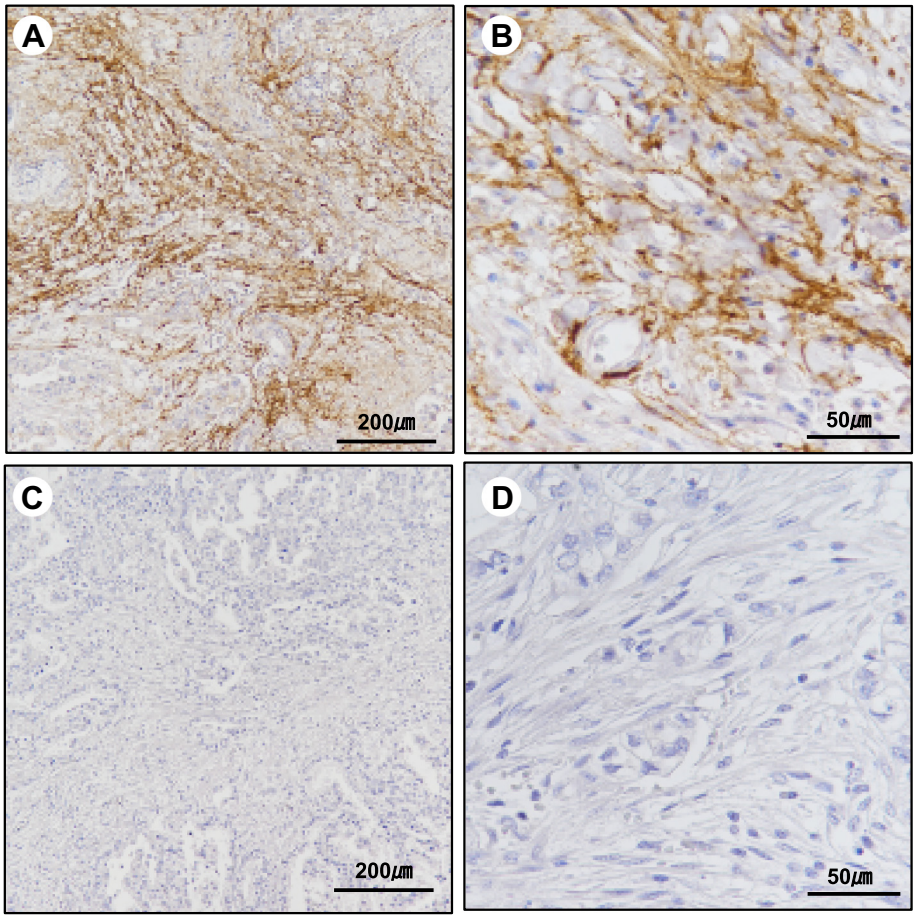

Fig. 7 Immunohistochemistry of fibulin-2 in the primary tumor (A and B) and Met-LNs (C and D) of the same patient with ICC. Immunoreactivity for fibulin-2 was found in the stroma of primary sites (A and B) but not in the cancer stroma of Met-LNs (C and D). Original magnifications ×100 (A and C) and ×400 (B and D).

Met-LN-CAFs were positive for α-SMA, PDGFR-β, and Thy-1 but negative for fibulin-2 and fascin. This expression pattern is not the same as that of ICC-CAFs. In 6 cases for which both primary site and the Met-LNs had been preserved, fibulin-2 immunoreactivity was found in the stroma at the primary sites but not in that of the Met-LNs. These data suggest that ICC-CAFs at the primary sites may not be a cellular source of Met-LN-CAFs but instead possibly derived from resident fibroblastic cells in LNs.

5. Conclusions

The immunohistochemical features of ICC-CAFs more closely resembled those of PFs than HSCs. BMDFs may contribute to the ICC-CAF population. In Met-LNs, CAFs were found to be present, and 3 types of morphology in their aggregation were found. Based on the molecular expression pattern of Met-LN-CAFs, their cellular source may be from fibroblastic cells residing in the LNs.

Supplementary data

Supplementary data to this article can be found online at https://doi.org/10.1016/j.humpath.2018.08.016.

Acknowledgment

We thank K. Mitani for her skillful assistance with the immunohistochemistry.

References

[1] Wang H, Liu W, Tian M, et al. Coagulopathy associated with poor prognosis in intrahepatic cholangiocarcinoma patients after curative resection. Biosci Trends 2017;11:469-74.
[2] Noguchi H. Macroscopic classification and prognotic factors of intrahepatic cholangiocarcinoma. J Jpn Surg Assoc 1999;60:1751-5.
[3] Sirica AE, Gores GJ. Desmoplastic stroma and cholangiocarcinoma: clinical implications and therapeutic targeting. Hepatology 2014;59:2397-402.

[4] Sirica AE. The role of cancer-associated myofibroblasts in intrahepatic cholangiocarcinoma. Nat Rev Gastroenterol Hepatol 2011;9:44-54.
[5] Zhang XF, Dong M, Pan YH, et al. Expression pattern of cancer-associated fibroblast and its clinical relevance in intrahepatic cholangiocarcinoma. Hum Pathol 2017;65:92-100.
[6] Santi A, Kugeratski FG, Zanivan S. Cancer associated fibroblasts: the architects of stroma remodeling. Proteomics 2017;6:392-401.
[7] Kalluri R. Fibroblasts in cancer. Nat Rev Cancer 2006;6:392-401.
[8] Shiga K, Hara M, Nagasaki T. Cancer-associated fibroblasts: their characteristics and their roles in tumor growth. Cancer 2015;7:2443-58.
[9] Gascard P, Tlsty TD. Carcinoma-associated fibroblasts: orchestrating the composition of malignancy. Genes Dev 2016;30:1002-19.
[10] Orimo A, Weinberg RA. Heterogeneity of stromal fibroblasts in tumors. Cancer Biol Ther 2007;6:618-9.
[11] Yamamura Y, Asai N, Enomoto A, et al. Akt-Girdin signaling in cancer-associated fibroblasts contributes to tumor progression. Cancer Res 2015;75:813-23.
[12] Shimoda M, Mellody KT, Orimo A. Carcinoma-associated fibroblasts are a rate-limiting determinant for tumor progression. Semin Cell Dev Biol 2010;21:19-25.
[13] Xing F, Saidou J, Watabe K. Cancer associated fibroblasts (CAFs) in tumor microenvironment. Front Biosci (Landmark Ed) 2010;15:166-79.
[14] Ishii G, Ochiai A. The origin of fibroblast recruited into cancer-induced stromal tissue. Kenbikyou 2008;43:104-9.
[15] Niinami C, Hayashi N. Use of multiple marker for in vivo characterization and quantitation of hepatic stellate cells in experimental and human liver cirrhosis. J Tokyo Womens Med Univ 2000;70:702-12.
[16] Wells RG. The portal fibroblast: not just a poor man's stellate cell. Gastroenterology 2014;147:41-7.
[17] Uyama N, Iimuro Y, Kawada N, et al. Fascin, a novel marker of human hepatic stellate cells, may regulate their proliferation, migration, and collagen gene expression through the FAK-PI3K-Akt pathway. Lab Invest 2012;92:57-71.
[18] Strieter RM, Keeley EC, Burdick MD, Mehrad B. The role of circulating mesenchymal progenitor cells, fibrocytes, in promoting pulmonary fibrosis. Trans Am Clin Climatol Assoc 2009;120:49-59.
[19] Sirica AE, Campbell DJ, Dumur CI. Cancer-associated fibroblasts in intrahepatic cholangiocarcinoma. Curr Opin Gastroenterol 2011;27:276-84.
[20] Okabe H, Beppu T, Hayashi H, et al. Hepatic stellate cells may relate to progression of intrahepatic cholangiocarcinoma. Ann Surg Oncol 2009;16:2555-64.
[21] Matsuwaki R, Ishii G, Zenke Y, et al. Immunophenotypic features of metastatic lymph node tumors to predict recurrence in N2 lung squamous cell carcinoma. Cancer Sci 2014;105:905-11.
[22] Kwak Y, Lee HE, Kim WH, Kim DW, Kang SB, Lee HS. The clinical implication of cancer-associated microvasculature and fibroblast in advanced colorectal cancer patients with synchronous or metachronous metastases. PLoS One 2014;9:e91811.
[23] Rozenchan PB, Pasini FS, Roela RA, et al. Specific upregulation of RHOA and RAC1 in cancer-associated fibroblasts found at primary tumor and lymph node metastatic sites in breast cancer. Tumour Biol 2015;36:9589-97.
[24] Mundim FG. Metastatic lymph node fibroblasts maintain similar profile of stromal biomarkers registered in primary breast carcinomas. Cancer Res 2015;75:4-24.
[25] Duda DG, Duyverman AM, Kohno M, et al. Malignant cells facilitate lung metastasis by bringing their own soil. Proc Natl Acad Sci U S A 2010;107:21677-82.
[26] Yeung TM, Buskens C, Wang LM, Mortensen NJ, Bodmer WF. Myofibroblast activation in colorectal cancer lymph node metastases. Br J Cancer 2013;108:2106-15.
[27] Motoyama H, Komiya T, Thuy le TT, et al. Cytoglobin is expressed in hepatic stellate cells, but not in myofibroblasts, in normal and fibrotic human liver. Lab Invest 2014;94:192-207.
[28] Shigaki S. Clinical and pathological studies on metastasis to the cervical lymph node of oral cancer. Jpn J Oral Maxillofac Surg 1979;25:784-97.
[29] Löhr M, Schmidt C, Ringel J, et al. Transforming growth factor-beta1 induces desmoplasia in an experimental model of human pancreatic carcinoma. Cancer Res 2001;61:550-5.